Modeling the Buildup of Polyelectrolyte Multilayer Films Having Exponential Growth[⊗]

Philippe Lavalle,[†] Catherine Picart,[†,‡] Jérome Mutterer,[§] Csilla Gergely,[†] Howard Reiss,[#] Jean-Claude Voegel,[†] Bernard Senger,[†] and Pierre Schaaf*,[⊥]

Institut National de la Santé et de la Recherche Médicale, Unité 595, Faculté de Chirurgie Dentaire, Université Louis Pasteur, 11 rue Humann, 67085 Strasbourg Cedex, France, Ecole Européenne de Chimie, Polymères et Matériaux de Strasbourg, 25 rue Becquerel, 67087 Strasbourg Cedex 2, France, Institut de Biologie Moléculaire des Plantes, 12 rue du Général Zimmer, 67084 Strasbourg Cedex, France, Department of Chemistry and Biochemistry, University of California, Los Angeles, California 90095-1569, and Institut Charles Sadron, Centre National de la Recherche Scientifique, Université Louis Pasteur, 6 rue Boussingault, 67083 Strasbourg Cedex, France

Received: June 19, 2003; In Final Form: September 19, 2003

Two types of polyelectrolyte multilayer films have been reported in the literature. These are (i) films whose mass and thickness increase linearly as the number of deposited bilayers increases and (ii) films that grow exponentially. We present a model for the buildup of exponentially growing films that allows a discussion of the behavior of them in a unified manner. This model is based on the diffusion both in and out the whole film of part of the chains of at least one of the polyelectrolytes constituting the multilayer. In short, the film is brought into contact with the solution of polyelectrolytes that are able to diffuse into the film. Inside of the film, chains of this polyelectrolyte constitute the "free" chains. At the subsequent rinsing step, some of them diffuse outward from the film. The remaining chains leave the film as it is brought into contact further with the polyelectrolyte solution of opposite charge. As the "free" chains reach the film/solution interface, they are complexed by the polyelectrolytes of opposite charge. These complexes, which are composed of both types of polyelectrolytes, contribute to the formation of the additional mass of the multilayer. The model relies on the evaluation of the electrostatic potential in the film within the framework of the Debye−Hückel approximation and takes into consideration the Donnan effect, which is due to noncompensated fixed charges in the film. It also includes the situation where none of the polyelectrolytes diffuse within the multilayer, in which case the film grows linearly. The model predicts the existence of a free-energy barrier that prevents total diffusion of any "free" polyelectrolyte outward from the film during a rinsing step, following contact with a polyelectrolyte solution. It also predicts that usually only one of the two polyelectrolytes that comprise the film diffuses readily into it. Both polyelectrolytes that comprise the film can diffuse "into" and "out of" the multilayer only when the concentration of noncompensated fixed charges within the film is very small. Several predictions of the model are discussed in the light of experimental results that have already been published or are new.

I. Introduction

When a solution of polyelectrolytes (e.g., polycations) is brought into contact with a negatively charged solid surface, polycations adsorb on the substrate. The adsorption process is generally irreversible and usually leads to charge overcompensation, so that the surface charge becomes positive. When this coated surface is brought into contact with a polyanion solution, the polyanions interact with the adsorbed polycations. This leads again to charge overcompensation and, thereby, to the appearance of a negative surface charge, as demonstrated by the variation of the zeta potentials (ζ) of surfaces of colloidal particles[1] or capillaries[2] that have been brought alternately into contact with polyanion and polycation solutions. The repetition of this alternating deposition process leads to the buildup of a multilayer polyelectrolyte film.[3] These multilayer films suggest possible applications in fields as different as electroluminescent photodiodes[4,5] or biomaterials.[6−10] The elucidation of their mechanism of buildup has been the focus of many recent experimental[11−18] and theoretical studies.[19−22]

In most of the early works in this field, the main feature of the build-up process was the interaction of polyelectrolytes from the solution with polyelectrolytes of opposite charge forming the upper layer of the film, rather than the interaction of solution polyelectrolytes with the underlying layers, as a result of deep penetration.[3,23,24] As a consequence, both the thickness and the mass of the film increase in proportion to the number of deposited polyanion/polycation bilayers. Polystyrene sulfonate/polyallylamine hydrochloride (PSS/PAH) films constitute a typical example of such linear growth.[25−28] When the polyelectrolytes from the solution are restricted to interact with the outer layer of the film, the resulting architecture is characterized by a species periodicity along the direction perpendicular to the

[⊗] This article is dedicated to Professor Adrien Schmitt on the occasion of his 65th birthday.

* Author to whom correspondence should be addressed. E-mail: schaaf@ics.u-strasbg.fr.

[†] Institut National de la Santé et de la Recherche Médicale, Faculté de Chirurgie Dentaire, Université Louis Pasteur.

[‡] Ecole Européenne de Chimie, Polymères et Matériaux de Strasbourg.

[§] Institut de Biologie Moléculaire des Plantes.

[#] University of California, Los Angeles.

[⊥] Institut Charles Sadron, Centre National de la Recherche Scientifique, Université Louis Pasteur.

10.1021/jp035740j CCC: $27.50
Published on Web 12/12/2003

adsorbing surface. The period is on the order of a few nanometers, i.e., the typical thickness of one bilayer, as demonstrated by neutron reflection.[29,30]

The properties (e.g., the thickness) of linearly growing multilayer films can be finely tuned by controlling the growth conditions. In this respect, the ionic strengths of the polyelectrolyte solutions constitute a particularly important parameter, greatly influencing the thickness per deposited bilayer.[2,28,30] A high ionic strength leads usually to a large thickness and a large amount of adsorbed molecules per deposition cycle. Also, for weak polyelectrolytes, the pH of the solution has a major role in determining the thickness increment per deposited bilayer.[13,23] Local electrostatic interactions deep within a multilayer can also be dependent on the nature of the polyelectrolyte that forms the outer layer. For example, the ionization of a weak polyelectrolyte, embedded in a layer of strong polyelectrolytes, is dependent on the nature (polycation or polyanion) of the outermost layer of the film.[31] In addition to the influence of ionic strength and pH, both the molecular mass[32] and the charge density of the polyelectrolytes[33] also are important.

Recently, multilayer films whose thicknesses increase exponentially with the number of deposited bilayers have been reported.[9,15,16,18,28,34−39] For these systems, the film thickness can reach several hundreds of nanometers or even micrometers after only 10−20 deposition cycles. The mechanism responsible for this exponential growth cannot be explained solely by the interaction of polyelectrolytes from the solution with those that constitute the outer layer of the film. Exponential growth implies a deposition process such that the thickness of newly deposited material is proportional to the film thickness at the time of deposition. Our recent studies suggest that the mechanism of exponential growth is intimately related to the diffusion throughout the film of at least one of the polyelectrolytes that comprise the film. Such diffusion occurs "into" the film when it is brought into contact with the solution of polyelectrolytes able to diffuse into the film, and "out of" the film when it is brought into contact with the rinsing solution, as well as with the solution of polyelectrolytes of opposite charge, during each cycle of bilayer deposition.[16,36,40,41]

The aim of this article is to provide a model for the general case where the polyelectrolytes interact directly with the outer layer of the film, as well as diffuse both "into" the multilayer film and "out of" it. This model is based mainly (i) on the electrostatic barrier formed at the film/solution interface during contact of the film with a polyelectrolyte solution, and (ii) on the difference in electrochemical potentials between the polyelectrolytes in the film and in the solution, in part because of electrostatic interactions within the multilayer. The latter contribute also to the interfacial energy barrier. Ultimately, the properties of the film are dependent, to a large extent, on the interplay of these phenomena.

The paper is organized as follows. First, Section II summarizes the experimental techniques that we have used to follow the growth process. Section III describes experiments performed, with the purpose of providing the essential ideas used as guidelines in the elaboration of the model. Section IV demonstrates that the exponential growth observed with some films may be explained in terms of the hypothesis of the polyelectrolyte diffusion mentioned previously. Section V contains a theoretical analysis of the fundamental features that likely result in the experimental observations. In particular, they form the basis for a discussion of the possible origin of the presence or absence of the diffusion "into" and "out of" the film during growth. In this way, the various behaviors of the films, as revealed by the experiments, can be rationalized. This is illustrated especially in Section VI in terms of the new experimental findings. Concluding remarks are presented in the last section. Details of the theoretical analysis, which are omitted in Section V, are furnished in the Appendix.

II. Experimental Methods

Polyelectrolytes. The polyelectrolytes used were poly (L-lysine) (PLL, molecular weight (Mw) of 30 300, from Sigma), poly (L-glutamic acid) (PGA, Mw = 72 000, from Sigma), hyaluronan (HA, Mw = 400 000, from BioIberica, Barcelona, Spain) and polyethylenimine (PEI, Mw = 70 000, from Polysciences, Warrington, PA).

Optical Waveguide Lightmode Spectroscopy (OWLS). The $(PLL/HA)_i$ and PEI−$(PGA/PLL)_i$ film build-up processes were followed by optical waveguide lightmode spectroscopy (OWLS). Briefly, OWLS is an optical technique in which an evanescent wave senses the film. The technique is sensitive to the film structure over a distance of the order of the penetration depth of the evanescent wave near the waveguide surface (over ∼200−300 nm). It gives access to the effective refractive index for transverse electric (N_{TE}) and magnetic (N_{TM}) polarization, from which the optical properties of the films can be derived.[42,43] Details of the experimental setup and the analysis of the optical data can be found elsewhere.[16] Qualitatively, N_{TE} and N_{TM} are proportional to the amount of material adsorbed on the surface. Therefore, increases in the magnitudes of these raw signals indicate increases in the masses that have been adsorbed. This is true for films whose thickness is less than ∼300 nm. For thicker films, the raw N_{TE} and N_{TM} signals are not sensitive to the mass adsorbed on top of the film, but they are sensitive to the structural changes that occur in the vicinity of the waveguide surface (up to ∼300 nm). An increase of the refractive index of the film usually leads to an increase of both N_{TE} and N_{TM}. The experiments described here are focused on this second regime of the signal.

PLL was first adsorbed by injection into the OWLS cell for 12 min, after which point the PLL solution was removed by rinsing with a 0.15 M NaCl solution (pH ∼6.5). HA was then deposited and rinsed after 12 min using the same procedure. In the same way, the alternate deposition of PLL and HA was continued.

Quartz Crystal Microbalance (QCM). A quartz crystal microbalance (Q-Sense, Götenborg, Sweden), denoted as QCM, was also used as a complementary technique to check the film build-up process. It involves the measurement of the change in the resonance frequency (Δf) of a quartz crystal[44] as material is deposited on it.[45] The resonance frequency shifts are measured when the crystal is excited at its fundamental frequency (∼5 MHz) and at the third, fifth, and seventh overtones (denoted as ν). An algebraic decrease in $\Delta f/\nu$ is usually associated, in a first approximation, to an increase in the mass coupled to the quartz.

Confocal Laser Scanning Microscopy (CLSM). For the study using CLSM, the PLL/HA multilayers were deposited on borosilicate glass slides (LabTek Chamber, Polylabo, France) following the same procedure as that described previously for OWLS. The dye-conjugated polyelectrolytes (HA-TR (Texas Red) and PLL-FITC (Fluorescein isothiocyanate)) were adsorbed in the same way at a certain stage of the build-up process.[16] CLSM observations were performed with a Zeiss model LSM 510 microscope using a 63×, 1.4 N.A. oil immersion objective and 0.4-μm z-section intervals. Virtual vertical sections can be visualized and allow the thickness of the film to be determined.

CLSM was also used to perform fluorescent recovery after photobleaching (FRAP) measurements. A rectangular zone was

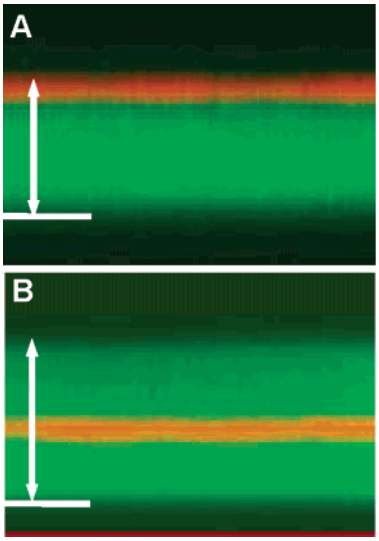

Figure 1. Vertical sections through different (PLL/HA) film structures (PLL and HA at 1 mg/mL diluted in 0.15 M NaCl solution) that contain labeled polyelectrolyte layers (red, HA-TR; green, PLL-FITC) obtained by confocal laser scanning microscope (CLSM) observations. White line indicates the borosilicate substrate (bottom of the chamber). Panel A shows a $(PLL/HA)_{19}-PLL_{20}$ multilayer film with two labeled layers, i.e., $PLL_{19}-FITC$ and $HA_{19}-TR$; the image size is 11.8 μm × 8.4 μm, and green fluorescence (corresponding to PLL-FITC) is visible over a total thickness of ~4 μm (white arrow). Panel B shows a $(PLL/HA)_{25}$ multilayer film with two labeled layers, i.e., $PLL_{19}-FITC$ and $HA_{19}-TR$; the image size is 20.2 μm × 14.4 μm, and green fluorescence is visible over a total thickness of ~8.0 μm (white arrow).

bleached. The fluorescence intensity of the bleached zone was then measured at different times.[46] The ratio of the intensity of the bleached zone to the intensity of the nonbleached zone gives the proportion of fluorescently labeled chains that are mobile in the film.

III. Experimental Basis for the Development of a Model for the Build-Up Mechanism

As mentioned in the Introduction, the existence of the inward and outward diffusion mechanism seems to be of primary importance in the attempt to understand the formation of an exponentially growing multilayer. The present section is focused on reporting the experimental observations of this process, as well as suggesting the essential physical parameters that might be responsible for the most striking features of various examples of exponential growth.

PLL/HA Multilayer. Inward and outward diffusion has been demonstrated for the PLL/HA system by CLSM fluorescence. By incorporating PLL labeled with fluorescein isothiocyanate (FITC, a green probe) and HA labeled with Texas Red (TR, a red probe) in the film at various steps of its buildup, it was observed that HA does not diffuse throughout the film, whereas PLL does. A $(PLL/HA)_{20}$ multilayer film has been constructed with solutions that contain 0.15 M NaCl. The film, where PLL−FITC has been used for the last step, appears entirely green, indicating that PLL−FITC is present throughout the entire structure (Figure 1A). Moreover, a $(PLL/HA)_{25}$ film in which $PLL_{19}-FITC$ and $HA_{18}-TR$ have been inserted also appears entirely green (Figure 1B).

These observations can be explained as follows. As the film is brought into contact with the PLL−FITC solution, these chains diffuse into the film and constitute the "free" chains. In the film, they can, however, partially exchange with nonlabeled PLL chains that are part of the PLL/HA network forming the

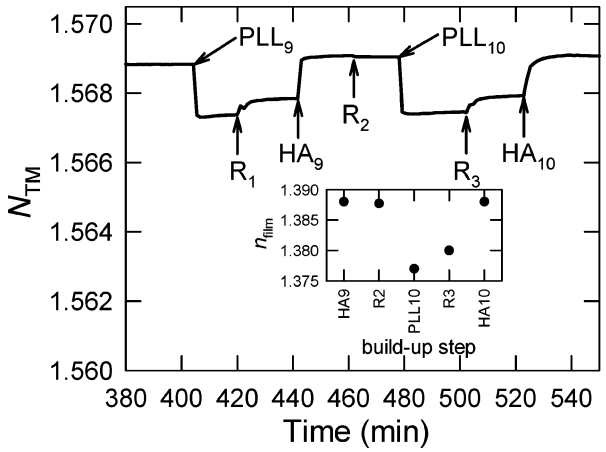

Figure 2. Effective refractive index (N_{TM}) signal obtained by OWLS during a (PLL/HA) multilayer buildup, as a function of time (PLL at 20 mg/mL and HA at 1 mg/mL diluted in 0.15 M NaCl solution). The development of the N_{TM} signal is shown over two build-up cycles, after a continuous film is formed on the surface. Each arrow corresponds to the beginning of the injection of either HA or PLL or to a rinsing step denoted by R_1, R_2, or R_3. The number beneath PLL or HA corresponds to the layer-pair deposition number. The inset in the figure represents the behavior of the refractive index of the film (n_{film}) near the waveguide at the end of each deposition step during one build-up cycle.

multilayer; the total concentration of "free" polyanion chains remains constant in the film during this process. During the rinsing step, some of these "free" chains diffuse out of the film. As the multilayer is further brought into contact with the HA solution, the remaining "free" polyanions (i.e., both PLL−FITC and PLL chains) diffuse out of the film. As they reach the film/solution interface, they are complexed by the HA chains and form PLL/HA and PLL−FITC/HA complexes that contribute to the formation of the additional mass of the multilayer. This observation explains why the entire $(PLL/HA)_{18}-(PLL-FITC/HA-TR)$ film appears green. When the build-up process is continued on this film with nonlabeled PLL, each time that PLL diffuses into the film, some of these new "free" chains can again exchange with the PLL−FITC chains previously incorporated, so that the subsequently added material also appears green.

A second proof of the existence of mobile PLL chains in the film was obtained recently. A rectangular zone with an area of 130 μm × 31 μm in a $(PLL/HA)_{34}-PLL-FITC$ film was bleached and the fluorescence recovery was followed.[46] Only 65% of the fluorescence intensity was recovered at long times in the bleached zone. This proves that 65% of the PLL−FITC chains remain "free" in the film but that 35% have exchanged with chains that can be considered as fixed. These chains are expected to be those that are engaged in the PLL/HA complexes that form the film.

OWLS provides a third, although more indirect, proof for the diffusion process. As already discussed, this technique only senses a zone that extends ~200−300 nm from the waveguide surface. Consequently, when the film thickness exceeds this penetration length, the film behaves as an infinite medium. Therefore, the technique should become insensitive to the addition of polyelectrolytes, after the film thickness exceeds the detection threshold. Thus, it is expected that the optical signals should become constant. In fact, one observes, for exponentially growing films, that the value of N_{TM} averaged over a build-up cycle (contact with polycation solution, followed by rinsing plus contact with polyanion solution, followed by rinsing) becomes constant from cycle to cycle (Figure 2). However, significant variations are observed within a cycle.

Figure 2 illustrates a typical example of the evolution of N_{TM} over two build-up cycles for the PLL/HA system, after a thick film has been formed (thickness of ~1 μm, as measured by atomic force microscopy (AFM),[15] after the deposition of eight PLL/HA bilayers). The changes in optical signal observed during the different steps of film construction reveal variations of the refractive index of the film in the vicinity of the film/waveguide interface (i.e., up to 200−300 nm from the solid surface). Such changes can originate from inward and outward polyelectrolyte diffusion through the film/solution interface that propagates throughout the entire film.

The evolution of the signal in Figure 2 may be interpreted as follows. When a PLL/HA film is brought into contact with PLL solution, free PLL chains diffuse into the film, leading to the observed decrease of the refractive index (see inset in Figure 2). This decrease of refractive index may be due to a film swelling. When buffer replaces the PLL solution, the optical signal increases to the extent that ~30% of the initial signal decrease is recovered. In the meantime, the film refractive index increases (see inset), which suggests partial diffusion of PLL out of the film, probably accompanied by a deswelling of the film. When the film is put in contact with the HA solution, after this rinsing step, the optical signal increases further until it reaches the level attained prior to the original PLL addition. The rinsing step that occurs following contact with HA hardly alters the N_{TM} signal. This shows that the behavior of HA is completely different from that of PLL. Thus, N_{TM} increases during contact with the HA solution, whereas it decreases when the multilayer is in contact with the PLL solution. All these observations are compatible with the findings obtained with CLSM, indicating that PLL diffuses inward and outward, in contrast to HA, which is adsorbed at the interface without penetration into the film.

One might object that the cyclic evolution could have been explained by a dissolution/reconstruction mechanism. However, this scenario can be excluded using the QCM. The frequency shift measured during the formation of the film decreases steadily and exponentially as the film construction progresses, even in the domain where optical signals vary cyclically. This finding indicates a continuous increase of the mass accumulating on the crystal. If dissolution were involved, the frequency decrease would not be monotonic.[15]

PGA/PAH Multilayer. PGA/PAH is another system that grows exponentially.[40] OWLS and Fourier transform infrared (FTIR) spectroscopy show that PGA is the diffusing species and PAH does not diffuse. The diffusion of PGA chains into the film is, as in the former example, accompanied by a change of the N_{TM} signal. However, no optical signal evolution is observed during the rinsing step that follows contact with PGA.[40] Thus, free PGA chains do not seem to diffuse out of the film during the rinsing step. Moreover, FTIR shows that the secondary structure of the multilayer was similar throughout the multilayer.

PGA/PLL Multilayer. Thus far, we have described exponential buildup in which only one of the polyelectrolytes diffuses "into" and "out of" the entire film. Figure 3 shows the evolution of the N_{TM} signal in the cyclic regime for a film that has been formed with PGA and PLL on a precursor layer of PEI.[36] The buffer used for polyelectrolyte dissolution and rinsing solution was MES-Tris (MES 25 mM, Tris 25 mM, pH 7.4) that contained 0.10 M NaCl. As noted previously, in the cyclic phase, OWLS cannot determine the thickness of the film because it is larger than the effective range of the method, i.e., ~300 nm. On the other hand, note that, in Figure 3, where the contact

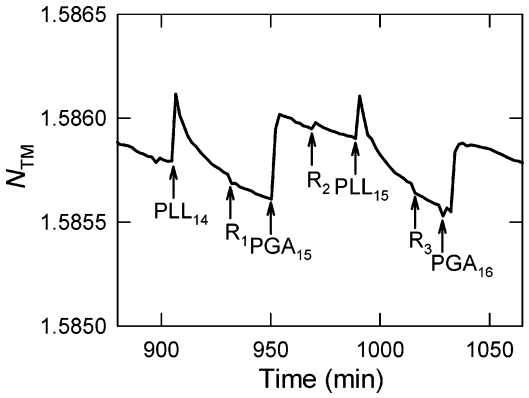

Figure 3. Effective refractive index (N_{TM}) obtained by OWLS during a (PGA/PLL) multilayer buildup, as a function of time. The evolution of N_{TM} is shown over two build-up cycles after a thick film is formed on the surface. Each arrow corresponds to the beginning of the injection of either PGA or PLL or to a rinsing step denoted by R_1, R_2, or R_3. The number beneath PLL or PGA corresponds to the layer-pair deposition number. The buffer used for polyelectrolyte dissolution and rinsing solution was MES-Tris (MES 25 mM, Tris 25 mM, pH 7.4) that contained 0.10 M NaCl.

and rinsing times were fixed to 15 min, the signal does not display a plateau. This shows that, in this film and for this experiment, equilibrium was never reached either after contact with a polyelectrolyte solution or after a rinsing step. In this case, the time of contact between film and solutions seems to be a particularly important parameter in the build-up process. For example, as the film is brought into contact with the polycation solution (see arrows labeled PLL_{14} and PLL_{15} in Figure 3), the N_{TM} signal first increases rapidly and then decreases at a slower rate. This shows that free polyanions contained in the film prior to contact with the PLL solution first diffuse "out of" the film. When the polyanions reach the film/solution interface, they come in contact with the polycations in the solution and should interact with them to form polyanion/polycation complexes. These complexes are then expected to form the new outer layer of the film. The diffusion of polyanions outward from the film prevents polycations from the solution from diffusing inward. When the concentration of free polyanions in the film becomes small enough and the buildup of the new outer layer has almost stopped, polycations start to diffuse "into" the film. Recent investigations using CLSM had already revealed that PLL diffuses through a PEI−$(PGA/PLL)_{16}$ multilayer film.[41] Diffusion of the polycations into the film must be slower than the diffusion outward from it because of the presence of remaining free polyanions with which the polycations can interact.[47] In contrast to what is observed for the PLL/HA and PGA/PAH systems, the N_{TM} signal still decreases during the rinsing step. This indicates that polycation chains continue to diffuse into the volume sensed by OWLS. Qualitatively, the same behavior is observed when polyanions are brought into contact with the film (see the region delimited by the arrows labeled "PGA_{15}" and "PLL_{15}" in Figure 3). This observation suggests that PGA also diffuses in the PGA/PLL multilayer film. Our recent observations using CLSM confirm this hypothesis (article in preparation). Therefore, the PGA/PLL film constitutes an example in which the two species of polyelectrolytes diffuse "into" and "out of" the film, although not necessarily with the same diffusion coefficient.

Simple Qualitative Analysis of the Experimental Observations on the PLL/HA, PGA/PAH, and PGA/PLL Systems. Most of the linearly growing films reported in the literature are prepared using highly charged polyelectrolytes, or polyelectro-

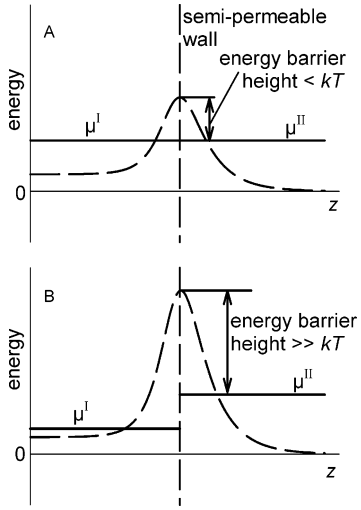

Figure 4. Scheme of the electrochemical potentials μ^{I} and μ^{II} (solid lines) of a polycation chain, as well as of the electrostatic energy barrier (dashed lines). Frame A concerns the case where the polycation flux stops when the electrochemical potentials in the two compartments (I and II) are equal. Frame B concerns the case where the energy barrier becomes so high that a chain from compartment II cannot surmount it to enter compartment I anymore. For details, see Section III.

lytes dissolved in solutions of low ionic strength.[3,13] Very often, these films are also dried after each deposition.[23] Such conditions should favor the formation of dense multilayers. It is then difficult or even impossible for a polyelectrolyte to diffuse into the film. In contrast, diffusion of a polyelectrolyte into the film may become possible when the structure of the multilayer is loose (or porous) on the nanometer scale. A second feature, which must be considered, is that polycation/polyanion charge compensation within the film is not systematically achieved. Thus "fixed" charges can exist in the multilayer.[1] To ensure electroneutrality (extrinsic compensation),[48] the "fixed" charges are compensated by the counterions present in the film. These counterions are in equilibrium with those in the solution and result in a Donnan effect. Ions can also be present in the film, because the multilayer is in contact with a salt solution, even though there is an exact compensation between the polycation and the polyanion charges. The absence of ions in the multilayer could thus only be due to the film's complete impermeability to them. This may be the case for films that grow linearly[11] and are dense in comparison to those into which a polyelectrolyte can diffuse.[49]

Hereafter, we shall describe an idealized system, which should help in the understanding of some of the features displayed by real film−solution and film-buffer systems. To this end, we consider a two-reservoir system. A semipermeable wall separates the two reservoir compartments, denoted as I and II, respectively (Figure 4). Particles can diffuse through this semipermeable wall and adsorb on it. Adsorption gradually renders the wall less permeable. Assume first that compartment II contains such particles diluted in water, whereas compartment I contains only water. If the wall is permeable, the particles diffuse from compartment II (infinite reservoir) to compartment I (finite reservoir). Thus, flux from compartment II to compartment I stops when μ^{I} (the chemical potential of a particle in compartment I) has reached the value μ^{II}, which is the chemical potential of a particle in compartment II, the latter being constant by design. Thus, in this system, the only regulating factor is the chemical potential of a particle. If molecules coming from compartment II do adsorb onto the wall, they gradually reduce its permeability. If the permeability decreases fast enough, the influx of molecules may be interrupted before $\mu^{I} = \mu^{II}$. The diffusion process then ceases when $\mu^{I} < \mu^{II}$. When pure water replaces the solution of particles in compartment II, μ^{II} drops suddenly to $-\infty$ (see eq 5 below). If the wall did not become impermeable in the former step, molecules leave compartment I until it is empty of them. The equality of the chemical potentials in both compartments is thereby recovered. On the other hand, if the wall became impermeable during the influx of particles, and if the adsorbed particles were not removed by the buffer, those that entered compartment I would be trapped and the system would then be characterized by $\mu^{I} > \mu^{II}$. Such simple reasoning already suggests that the state eventually reached by compartment I, whether in contact with a solution or pure water in compartment II, is dependent on both the chemical potentials and the possible blocking mechanisms at the interface separating compartment I from compartment II.

Now assume that the particles are polyelectrolytes (e.g., polycations, but the analysis is equally valid for polyanions). Their adsorption onto the wall may then reduce its permeability, not only by steric hindrance but also by the formation of an electrostatic barrier. In the case of our films, only this second effect is expected to have a role. The final state of the system then is dependent on the particle electrochemical potentials in compartments I and II and on the permeability of the wall. It should be emphasized that, generally, the solution in compartment II contains polyelectrolytes as well as ionized salt. The negative ions supplied by the salt (e.g., Cl^{-}) form a counterion cloud along the supposedly positively charged wall. The efficiency of the electrostatic repulsion of new incoming polycations due to the wall then also is dependent on the salt concentration of the solution in compartment II. Such an electrostatic barrier has its origin in the charge excess (see Appendix for an estimation of the electrostatic barrier, as a function of the charge excess) that appears after each polyelectrolyte deposition step. The existence of these charge excesses was proven by the evolution of the zeta potential (ζ) of the films during their buildup: this potential alternates between a positive and negative value after each polycation and polyanion deposition.[1,2] This potential can only originate from a charge excess that is located at the film/solution interface. If it would be smeared out over the entire film, the charges would be compensated by counterions in the film. Thus, these counterions would not be affected by the hydrodynamic flow used to sense the film potential and, thus, would not contribute to ζ.

As long as the energy barrier is not too high (for details and a rigorous approach, see Section V and the Appendix), diffusion over the barrier remains significant, and the polycations continue their penetration into compartment I. It is then possible for μ^{I} to reach the value of μ^{II}. Under these circumstances, the influx stops when the electrochemical potential equilibrium is achieved, despite the existence of an energy barrier (see Figure 4A). In contrast, if the energy barrier increases rapidly, the probability of passage of a polycation over it will tend rapidly to zero. The diffusion of polycations from compartment II to compartment I then ceases, even though $\mu^{I} < \mu^{II}$ (see Figure 4B).

In case A (Figure 4A), when the polyelectrolyte solution is replaced by water or buffer ($\mu^{II} \rightarrow -\infty$), the polycations can leave compartment I by recrossing the barrier toward compartment II. As they diffuse outward from the film, the concentration of polycations in the film decreases. Their electrochemical potential then decreases too. The diffusion out of the film continues up to a point where the difference between the height of the electrostatic energy barrier and the electrochemical potential becomes much larger than kT. At this point, the

outward diffusion ceases. Thus, one concludes that this outward diffusion stops before the film is totally empty of free polycations, as was observed experimentally. In contrast, in case B (Figure 4B), because the barrier eventually prevents the entrance of polycations into compartment I at a possible low level of μ^I, it prevents *a fortiori* the return of polycations to compartment II, because they would have to negotiate an even higher barrier. In both cases, after contact of the film with the polyanion solution, the electrostatic barrier disappears and is changed to an electrostatic sink. The "free" polycations remaining in the film then diffuse outward from it and are complexed by the polyanions as soon as they reach the film/solution interface. These complexes form the additional mass at the top of the film.

The discussion, thus far, has disregarded the possible presence of "fixed" charges within compartment I. As a consequence, the simple model presented previously suggests that the flux of polycations from compartment II to compartment I does not vanish until either (i) the electrochemical potentials are equal on both sides of the wall or (ii) the electrostatic interfacial barrier becomes too high. However, in compartment I, which is the compartment that represents the film in a real experiment, the "fixed" charges contribute to the electrochemical potential. If these charges are positive, the electrochemical potential of a polycation that might penetrate into compartment I would be increased, compared to its magnitude in the case where no "fixed" charges are present. It may therefore happen that no polycations penetrate into compartment I. The same scenario would hold for polyanions if the "fixed" charges were negative. Note that this particular blocking mechanism does not rely on an energy barrier that is concentrated at the wall, but rather on electrostatic repulsion extending over all of compartment I, which is due to the Donnan potential that builds up in the presence of fixed charges. This is the reason for the nonzero level of the barrier in compartment I (see Figure 4). The presence of "fixed" charges in compartment I reduces (or even forbids) the influx of either polycations or polyanions, depending on the sign of their charge. Conversely, when "fixed" charges are absent, both polycations and polyanions should be able to diffuse from compartment II to compartment I, i.e., from the solution into the film. For a quantitative evaluation of the barrier heights under various hypotheses, see eqs A13a, A13b, A19a, A19b, A25a, and A25b in the Appendix.

In regard to the buildup of a PLL/HA film, it has been shown (see previous discussion) that polycations (PLL) penetrate into the film and that some of them diffuse outward during rinsing. This shows that the energy barrier at the interface is low enough to allow outward diffusion. This interpretation leads to the conclusion that, preceding the rinsing step, the influx of PLL ceased because equality between the electrochemical potentials was attained. This situation is depicted by Figure 4A. After rinsing, contact of the film with the polyanion (HA) solution leads to the disappearance of the energy barrier that restricts PLL diffusion. Consequently, all free PLL chains, which remain in the film after rinsing, could diffuse outward.

In regard to the buildup of a PGA/PAH film, it has been shown (see previous discussion) that the polyanions (PGA) penetrate into the film but none diffuse outward during rinsing. This shows that (i) "fixed" charges prevent the polycations (PAH) from penetrating into the film, and (ii) the energy barrier at the interface is high enough to forbid the outward diffusion of PGA. This last point forces the conclusion that, preceding the rinsing step, the influx of PGA ceased because the barrier became too high. Thus, equality between electrochemical potentials was not attained. This situation is depicted by Figure 4B. After rinsing, the contact of the film with the polycation (PAH) solution leads to the disappearance of the energy barrier that opposes the movement of PGA. Consequently, free PGA chains trapped in the film can diffuse outward and are complexed with incoming PAH chains at the interface.

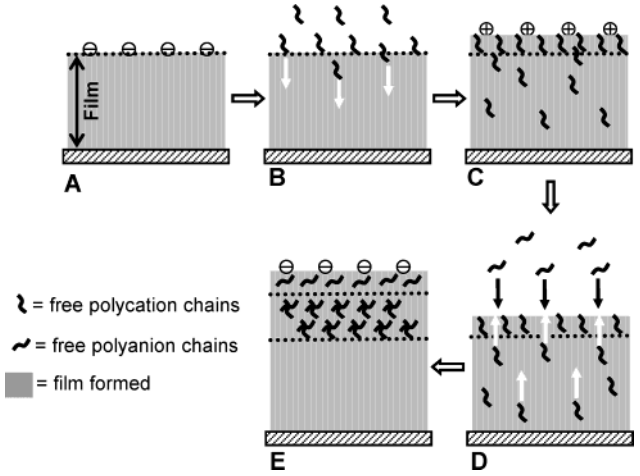

Figure 5. Schematic drawing of the build-up mechanism of a PLL/HA polyelectrolyte multilayer film, based on the diffusion of the polycation: (A) we assumed that the mechanism started with a negatively HA terminated film; (B) the film is put in contact with the polycation solution (PLL) (most of the chains diffuse "into" the film; some chains, however, adsorb on top of the film, leading to positive charge overcompensation in the film); (C) after a rinsing step, some free polycations remain in the film; (D) contact between the positively terminated film and the polyanion solution, followed by diffusion of the free polycation chains "out" of the film; (E) end of step D, resulting in negative charge overcompensation. The adsorption cycle results in a negatively terminated film thicker than that in step A.

In regard to the buildup of a PLL/PGA film, it has been shown (see previous discussion) that the polycations (PLL) and the polyanions (PGA) penetrate into the film. This shows that no "fixed" charges are present in the film, or at least that their concentration is small enough to have only a small effect. It was also inferred that equilibrium was not achieved in any of the build-up steps. This leads to the conclusion that, in our experiment, equality of electrochemical potentials was not attained, but, still, the barriers did not become too high during the contact and rinsing periods. It is therefore impossible to state whether this system would exhibit the behavior shown in panels A or B in Figure 4.

The experimental observations, discussed qualitatively previously, are analyzed in Section V and the Appendix on a more-quantitative, physical basis.

IV. Exponential Growth

As a consequence of the inward and outward diffusion processes postulated on the basis of the experimental results described in Section III, we can now suggest a mechanism for the buildup of a multilayer exhibiting exponential growth. An exponential growth law will be derived that contains linear growth as a special case.

Proposed Mechanism. A mechanism for exponential growth that was suggested earlier[16] is illustrated schematically in Figure 5 for the PLL/HA system previously described. When a film that has been terminated by a HA layer (Figure 5A) is brought in contact with the PLL solution (Figure 5B), polycations (PLL) diffuse throughout the entire multilayer down to the deposition substrate (Figure 5C). During the rinsing step that follows, some

of these polycations diffuse "out of" the film (see the discussion in Figure 4A). Polycations that remain in the film, after rinsing, diffuse "out of" the film during contact with the polyanion (HA) solution (see Figure 5D, 5E). In this step, the polycations are complexed by polyanions from the solution as soon as they reach the film/solution interface. These complexes form the new upper layer of the film (Figure 5E). The amount of newly deposited material is thus directly proportional to the number of polycations diffusing "out of" the film during its contact with the polyanion solution. Moreover, the number of film polycations diffusing to the interface is itself proportional, in first approximation, to the film thickness. It follows that the thickness grows exponentially. The postulated proportionality between newly deposited amounts of polyelectrolytes and film thickness requires that (i) the structure of the film be similar over the entire multilayer and (ii) all polycations diffusing outward from the film be complexed and participate in the formation of the new layer. The validity of the first requirement was recently demonstrated for the PGA/PAH system.[40] The importance of the second requirement will be discussed later.

Growth Law. After each rinsing step that followed the contact of the film with the polycation solution, for sufficiently long rinsing times, the concentration of free polycation chains that remain in the film can be assumed to be the same, regardless of the total thickness of the film. The number of free polycation chains that remain in a film formed of i bilayers is thus proportional to the film thickness and to the number $Q(i)$ of polyelectrolytes that comprise the film. When the film is brought into contact with the polyanion solution, all the free polycation chains that have not been eliminated by rinsing will diffuse outward from the film, to be complexed with polyanion chains to form the new outer layer. The number of polyelectrolytes that comprise this new outer layer, $\delta Q(i+1)$, is then the sum of two contributions. The first corresponds to the direct interaction of the polyelectrolytes from the solution with those that comprise the outer surface. This contribution may be denoted by q_0 and is responsible for the surface charge excess and should be constant, i.e., independent of i. The second contribution is proportional to the number of free chains in the film, and, hence, to $Q(i)$. It follows that $Q(i)$ satisfies the following difference equation:

$$\delta Q(i+1) = q_0 + KQ(i) \tag{1}$$

in which K is a proportionality constant. As $Q(i)$ increases with i, the second term on the right-hand side of eq 1 eventually becomes dominant. Assuming that no precursor layer (e.g., PEI) was deposited on the original surface, the initial condition then is $Q(0) = 0$. The general solution of eq 1 subject to this condition is given as

$$Q(i) = \frac{q_0}{K}(\exp(Ki) - 1) \tag{2}$$

As long as $Ki \ll 1$, i.e., depending on the value of K, out to a finite value of i, this relation reduces to $Q(i) \approx q_0 i$, which describes a film that grows linearly with the number of deposited bilayers. The special case of $K = 0$ occurs when no polyelectrolyte diffuses into the multilayer or when the polyanion/polycation complexes, which form at the film/solution interface as a result of the outward diffusion of the free polyelectrolytes, are not anchored to the multilayer. This effect is more or less similar to what has been observed by the Cohen-Stuart group in the poly(dimethylaminoethyl methacrylate)/poly(acrylic acid) system (PAMA/PAA).[50] On the other hand, for large K, $Q(i) \approx (q_0/K)\exp(Ki)$, which corresponds to an exponential growth. The simple formula shown in eq 2, which is itself based on a simple mechanism, is capable of describing both linear and exponential growth. It shows that the system can be made to evolve either linearly or exponentially for a given polyelectrolyte pair, if K can be altered by experimental conditions. Such behavior has indeed been observed for the PSS/PAH system, which remains linear over 10 bilayers[36] at weak ionic strength but shows an exponential trend over the first few bilayers when the salt concentration of the solutions exceeds 0.1 M.[28]

V. Modeling the Build-Up Process

In this section, we shall analyze the flux of polyelectrolytes, e.g., polycations, from the solution into the film, as well as the reverse flux during rinsing. This will demonstrate the major role of the electrochemical potentials in solution and film, and of the electrostatic energy barrier at the interface. We shall also derive the relation between polyelectrolyte concentration in the solution and that of free polyelectrolyte chains in the film. This will reveal the central importance within the film of fixed charges, arising from the lack of compensation of the charges of polycations and polyanions in the film.

Polycation Diffusion. Now consider just a single step of multilayer buildup. Assume that the polycation diffuses through the film, while the polyanion does not, which is a situation observed in the PLL/HA system (see Section III). Polyanion diffusion could be discussed in a similar manner. At the end of the rinsing step that follows polyanion adsorption, the outer surface of the film is negatively charged, as indicated by its negative ζ. When this film is brought into contact with the polycation solution, two processes occur simultaneously: (i) polycation chains interact with the negative outer layer, rendering the outer portion of the film positively charged, and (ii) other polycation chains diffuse into the film. Thus, as already indicated in Section III, during the adsorption process, an electrostatic energy barrier develops in the outermost portion of the film. The diffusion of polycation chains into the film can, in crude approximation, be described by the Smoluchowski equation:

$$\frac{\partial c}{\partial t} = \frac{\partial}{\partial z}\left[D\left(\frac{\partial c}{\partial z} + \frac{c}{kT}\frac{\partial \langle \Phi \rangle}{\partial z}\right)\right] \tag{3}$$

where c is the local polycation concentration, D the polycation diffusion coefficient, and $\langle \Phi \rangle$ the potential of mean force experienced by polycations in the film. The symbol k is the Boltzmann constant, T the absolute temperature, and t time. The variable $\langle \Phi \rangle$ consists of several contributions: (i) the electrostatic potential of the polycations within the film; (ii) a contribution $\langle \Psi \rangle_c$ that originates from the interaction of a free polycation and other free polycations, as well as with the multilayer network; and (iii) a contribution $\langle \Psi \rangle_e$ related to the elastic response of the film to the presence of the free polycations (swelling of the film as suggested by the observed decrease in refractive index; see Section III). It is expected that $\langle \Psi \rangle_c$ and $\langle \Psi \rangle_e$ increase with polycation concentration.

To acquire a qualitative understanding of the diffusion process, we assume that quasi-steady-state diffusion conditions are always reached very rapidly. In the following, the superscripts "f" and "s" denote quantities that refer to the film and solution, respectively (compare with compartments I and II in the simplified approach of Section III). Under quasi-steady-state conditions, the flux of polycation chains (J_0) is given by[51,52]

$$J_0 = -\frac{c^s \exp[(\langle\Phi\rangle^s - \langle\Phi\rangle_{max})/(kT)] - c^f \exp[(\langle\Phi\rangle^f - \langle\Phi\rangle_{max})/(kT)]}{\int_0^\delta (1/D(z)) \exp[(\langle\Phi(z)\rangle - \langle\Phi\rangle_{max})/(kT)]\, dz} \quad (4)$$

where $\langle\Phi\rangle_{max}$ represents the largest value of $\langle\Phi\rangle$ (top of the energy barrier) and δ is a distance much larger than the film thickness. Within the framework of a simple model based on the Debye−Hückel approximation, the electrostatic contribution to $\langle\Phi\rangle_{max}$ is proportional to A_s, as presented by eq A25b in the Appendix. Let us assume that the electrostatic contribution is the main contribution to $\langle\Phi\rangle_{max}$. The electrochemical potential of a polycation can be written as

$$\mu = \mu^0 + kT \ln c + \langle\Phi\rangle \quad (5)$$

where μ^0 is the translational contribution to the electrochemical potential. Equation 4 can then be rewritten as

$$J_0 = -L\left[\exp\left(\frac{\mu^s - \langle\Phi\rangle_{max}}{kT}\right) - \exp\left(\frac{\mu^f - \langle\Phi\rangle_{max}}{kT}\right)\right] \quad (6)$$

where L is a constant defined by comparison with eq 4, and μ^s and μ^f correspond to the electrochemical potentials of the polycation chains in the solution and in the film, respectively. As the polycation chains diffuse in the film, both $\langle\Phi\rangle_{max}$ and μ^f increase. The increase of barrier height seen from the solution, $\langle\Phi\rangle_{max}$, originates in two effects (see eq A25b). On one hand, the excess charge ρ^+ in the outer portion of the film increases, because of the adsorption of polycations. On the other hand, it may also increase, although at a slower rate, because the polycation concentration in the film, c^f, also increases. The polycation flux ceases when either the polycation electrochemical potentials in the film and solution become equal (see Figure 4A), or the barrier becomes so high that the polycations from the solution can no longer surmount it (Figure 4B).

During the rinsing step, the excess charge in the outer part of the film can be assumed to remain constant. This excess charge is due to outer polyelectrolytes that should strongly interact with the film network, and thus should not be removed during rinsing. At the beginning of this step, c^s becomes rapidly zero but c^f remains almost constant. Thus (see eq A25a), the barrier, as seen from the film, decreases slightly. In the simple present approach, these changes will be neglected. If the polycation flux into the film had ceased at the end of the former step because equilibrium between film and solution (Figure 4A) had been reached, then an outward polycation flux would occur during the rinsing step. This flux is given by

$$J_{out} = L \exp\left(\frac{\mu^f - \langle\Phi\rangle_{max}}{kT}\right) \quad (7)$$

The diffusion process of free polycation chains out of the film is accompanied by a decrease in μ^f. The amplitude of the energy barrier, as seen from the film, thus increases. Outward diffusion ceases when the barrier becomes too high, i.e., when $\langle\Phi\rangle_{max} - \mu^f \gg kT$, even though free polycation chains are still in the film. This is demonstrated by the fact that at the end of rinsing, the N_{TM} signal is smaller than before PLL injection. On the other hand, when the polycation flux into the film ceases because the barrier becomes too high, the quantity $\langle\Phi\rangle_{max} - \mu^f$ is even larger than the quantity $\langle\Phi\rangle_{max} - \mu^s$ (Figure 4B), so that no outward polycation flux occurs.[40] In both cases (panels A and B in Figure 4), when the film is brought in contact with the polyanion solution after rinsing, polyanion chains start to interact with the positively charged outer surface. Thus, the positive excess charge disappears and a negative charge appears. This causes a reversal of the electrostatic barrier, which now acts as a sink for free polycations located in the film. The free polycation chains thus diffuse toward the film/solution interface. As soon as they reach it, however, they are complexed by polyanions in solution near the film. When these polycation/polyanion complexes remain bound to the film, they form the new outer layer. This process continues until all free polycation chains have diffused out of the film, i.e., until they have been complexed, and charge overcompensation has led to a barrier, which is now repulsive for negative ions. Because all free polycations have been extracted from the film, the subsequent rinsing step does not change the film structure. At this stage, the build-up process of a bilayer is complete and the buildup of a new bilayer can start.

Concentration of Free Polyelectrolyte Chains. The concentration of free polyelectrolyte chains in the film can be derived as a function of chain concentration in solution when the diffusion of chains into the film ceases because equilibrium has been reached between the film and the solution ($\mu^f = \mu^s$). The free chain concentration in the film (c^f) is then related to the chain concentration in solution (c^s) (for details, see the demonstration leading to eq A28 in the Appendix) by

$$\varphi c^s \exp\left[\left(\frac{N^2}{2\varphi\rho_0}\right)\varphi c^s\right] = F c^f \exp\left[\left(\frac{N^2}{2\varphi\rho_0}\right)c^f\right] \quad (8)$$

where N is the number of charges carried by a polycation chain, φ corresponds to the available volume fraction of an ion in the film (in a crude way, the available volume corresponds to the volume accessible to an ion), ρ_0 is the salt (assumed to be NaCl) concentration in the solution, and F is a constant that is given by eqs A29 and A30:

$$F = \frac{\varphi}{\varphi'} \exp\left[(-1)^p\left(\frac{N\rho_{fc}}{2\varphi\rho_0}\right)\right] \quad (9)$$

where $p = 0$ for polycations and $p = 1$ for polyanions. In this expression, φ' corresponds to the available volume fraction for a chain (either polycation or polyanion) in the film. The parameter ρ_{fc} is the concentration of "fixed" charges in the multilayer film. These are due to the noncompensation between positive charges carried by polycations and negative charges carried by polyanions that comprise the film. The concentration ρ_{fc} has the sign of the "fixed" charges. Because N can be quite large (≥ 100), F can be very sensitive to ρ_{fc}. It should be stressed that the derivation of eqs 8 and 9 relies on several approximations:

(1) The electrostatic interactions are determined within the Debye−Hückel approximation.

(2) Volume exclusion interactions between free chains in the film, as well as the elastic response of the film due to the presence of the free chains, are neglected.

(3) The configurational entropy of the chains is assumed to be of the same order of magnitude in film and solution.

Equation 8 can be solved numerically for c^f (without approximation) for different values of F. Figure 6 shows the dependence of c^f on φc^s for different values of F, for the case of diffusing polycations. The fact that the value of c^f does not stabilize at high concentrations of the solution stems from the fact that interpolycation interactions in the film have been neglected. Small values of F correspond to the case of negative

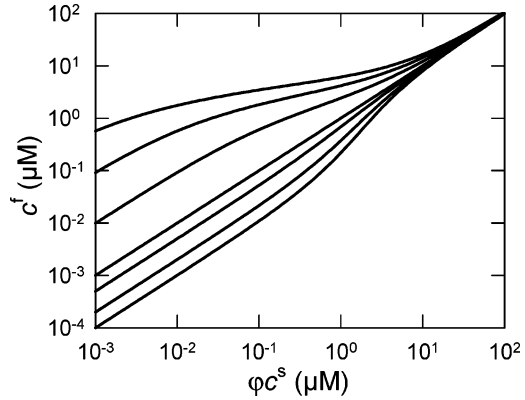

Figure 6. Evolution of the concentration of polycation in the film (c^f), as a function of φc^s (where c^s is the concentration of the polycation in the solution and φ is the available volume fraction per ion) for various values of F, according to eq 8, with $N^2/(2\varphi\rho_0) = 10^6$ M^{-1}. From top to bottom: $F = 0.001$, 0.01, 0.1, 1, 2, 5, and 10.

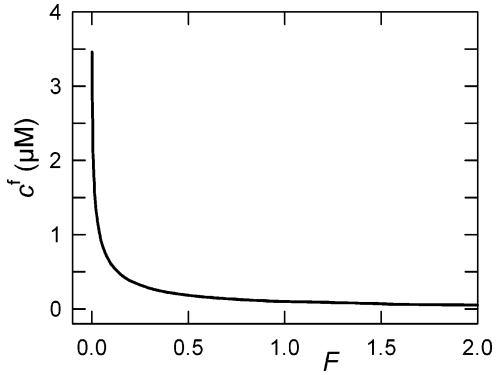

Figure 7. Behavior of c^f as a function of F for a polycation with $\varphi c^s = 0.1$ μM and $N^2/(2\varphi\rho_0) = 10^6$ M^{-1}, according to eq 8.

"fixed" charges that are expected to favor the inward diffusion of polycations. For large values of F, very few polycations diffuse into the film, because they are repelled by positive "fixed" charges. The dependence of c^f on F for fixed φc^s is shown in Figure 7, which illustrates the great sensitivity of free chain concentration to "fixed" charges in the film. Also implied is the fact that diffusion of both polyanions and polycations (see the example of the PGA/PLL film in Section III) can only be observed if the "fixed" charge concentration in the multilayer is almost zero. If this condition is not fulfilled, one of the polyions is prevented from penetrating into the film.

VI. Discussion of New Experimental Results in the Light of the Model

The central assumption of the model is that at least one of the polyelectrolytes that comprise the multilayer diffuses within the film when it is brought in contact with the polyelectrolyte solution. This has been verified by two different experimental approaches, as described in Section III. At equilibrium between the interior and the exterior of the multilayer, i.e., for $\mu^f = \mu^s$, our model suggests that the concentration of free polycation (polyanion) in the film increases as the polycation (polyanion) concentration in the solution increases, in accordance with eqs 8 and 9 or eqs A28−A30 in the Appendix. However, after rinsing, the residual polycation (polyanion) concentration should be independent of the concentration of the solution originally brought into contact with the film, because this residual concentration is dependent only on the height of the energy barrier seen from the film (see eq A25b in the Appendix, with $c^s = 0$). This prediction has been checked for thick (~1 μm) (PLL/HA) films when the OWLS signal becomes cyclic (Figure 8). For the sake of simplicity, the following shorthand notation is used: PLL-1 and PLL-20 refer to PLL solutions whose concentrations are equal to 1 and 20 mg/mL, respectively.

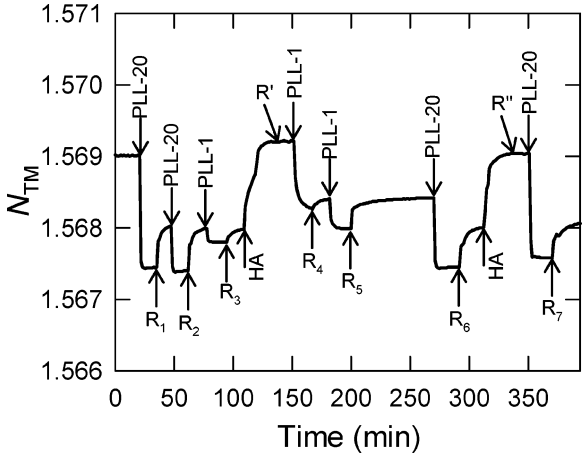

Figure 8. Effective refractive index (N_{TM}) obtained by OWLS during a PLL/HA multilayer buildup, as a function of time, after the cyclic regime was attained. A $(PLL/HA)_{10}$ film was first formed with HA at 1 mg/mL (PLL-1) and PLL at 20 mg/mL (PLL-20). The film was then brought into contact with PLL-20, followed by rinsing with a buffer (R_1), a second contact with PLL-20, a second rinsing (R_2), contact with a 1 mg/mL PLL solution, and a final rinsing (R_3). The film was then brought into contact with a HA solution and a similar PLL deposition and rinsing sequence was repeated but PLL-20 solutions were replaced by PLL-1 solutions and vice versa. The rinsing steps R_4, R_5, and R_6 successively follow contacts with PLL. Finally, the film was brought into contact with a HA solution, rinsed, and then brought in contact with PLL-20.

A $(PLL/HA)_{10}$ film, which has been built-up with PLL at 20 mg/mL and HA at 1 mg/mL, is first brought into contact with PLL-20, followed by rinsing with buffer (R_1), followed by a second contact with PLL-20 and a rinsing (R_2), and followed by a contact with PLL-1 and a final rinsing (R_3). The value of the N_{TM} signal (see Figure 8) after contacts with PLL-20 is less than its value after contact with PLL-1, indicating that, in the latter case, the concentration of free PLL chains in the film is smaller, as predicted by the model (see eqs 8 and 9). Moreover, the N_{TM} signals after each of the three rinsing steps are identical, within experimental error. This clearly shows that the concentration of free PLL chains that remain in the film after the three rinsing steps R_1, R_2, and R_3 is independent of the concentration of free chains in the film before rinsing. This is also in accordance with one of the predictions of the model, namely that the parameter that regulates the residual free chain concentration is the energy barrier seen from the film rather than the concentration within the film prior to rinsing.

The film is then brought into contact with a HA solution and rinsed (R′). A six-step sequence is then initiated, consisting of successive contacts with PLL-1, buffer (rinsing R_4), PLL-1, buffer (rinsing R_5), PLL-20, and buffer (rinsing R_6). This sequence is analogous to the first six-step sequence, except that PLL-20 replaces PLL-1 and vice versa. The first observation is that the values of the N_{TM} signals are the same after rinsings R_4 and R_5, although the signals before rinsing are different. This seems to confirm the observation that was made previously. However, the value of the N_{TM} signal is appreciably larger than it was after rinsings R_1, R_2, and R_3 and larger than it will be after contact with PLL-20 and rinsing R_6. This result is in conflict with the prediction of the model, which seemed to be

nicely verified until this point. Nevertheless, it is remarkable that, after rinsing R_6, the N_{TM} signal recovers its common value after rinsings R_1, R_2, and R_3. Moreover, the N_{TM} signal has the same value after the three contacts with PLL-20.

The departure from the predictions of the model could be due to structural film rearrangements and to hysteresis that follow swelling and deswelling induced by successive contacts with the polyelectrolyte solution and the rinsing solution. More precisely, when a film terminated by HA is brought in contact with a PLL-20 solution, the amount of PLL that diffuses into the film is larger than when it is brought into contact with a PLL-1 solution, as predicted by the model. Moreover, the diffusion of PLL into the film is accompanied by its swelling. This swelling must increase with the concentration of "free" PLL chains inside of the film. Thus, it is larger when the film is brought into contact with PLL-20, in comparison to contact with PLL-1. However, such a rapid swelling process must certainly also induce structural rearrangements inside of the film, which can be slow. Moreover, it is expected that they are smaller and slower for PLL-1 than for PLL-20, with the swelling state being less pronounced. During the rinsing step, only a portion of the PLL chains diffuse out of the film, so that deswelling is only partial. Thus, during the rinsing step that follows contact with a PLL-20 solution, the film does not relax to its initial state but instead remains in a swollen state. When this film is further brought into contact with a PLL-1 solution, the diffusion of PLL into the film acts on an already swollen state. On the other hand, when this film is then put in contact with the HA solution, all the "free" PLL chains diffuse out of the film and, thus, the film can recover the initial state that it had before the first contact with PLL-20. Then, when this film is put into contact with the PLL-1 solution, the swelling that accompanies the diffusion of PLL into the film is expected to be smaller than that for the preceding PLL-1 contact that followed the PLL-20 contact. This explains why the signal before rinsing R_4 is larger than the signal before rinsing R_3. Because the rearrangement is slow, especially if the PLL concentration inside of the film is small, it is expected that, when the film is further brought in contact with PLL-1 after rinsing R_4, a new PLL diffusion into the film induces further structural changes, so that the signal is smaller before rinsing R_5 than before rinsing R_4. Finally, when this film is brought into contact with PLL-20, the amount of PLL that diffuses into the film is much larger than during the PLL-1 contact. Thereby, the film loses the memory of the swelling state after PLL-1 and recovers the same state as before rinsing R_1. One can thus conclude that the discrepancies observed in Figure 8, with respect to the model, can be fully explained by structural rearrangements of the film, which are not included in that model and should be accounted for in a refined analysis.

VII. Conclusion

We have presented a model for the buildup of exponentially growing films, which allows a unified discussion of the behaviors of various polyelectrolyte systems. This model is based on an "inward" and "outward" diffusion process, throughout the entire film, of at least one of the polyelectrolytes that comprise the multilayer. It also relies on the existence of an energy barrier that prevents full diffusion of the polyelectrolytes outward from the film, during the rinsing step that follows contact with polyelectrolyte solution. It includes the case where none of the polyelectrolytes diffuse within the multilayer, i.e., the case of a linearly growing film. Several predictions of the model have already been observed in previous experimental investigations, whereas others have been confirmed by the new investigations reported here.

However, the proposed model does not answer all the questions. In particular, it fails to predict whether, on the basis of its chemical nature, a system will grow linearly or exponentially. Moreover, it is only semiquantitative, because it does not make allowance for the prediction of surface excess charge in the outer portion of the film. The model also neglects possible restructuring effects that are likely to occur within the film when it is swollen; such effects have been suggested by several experimental observations. All these issues require further investigation and refinement of this initial approach. Nevertheless, the model provides a simple scheme that accounts for most of the general observations that are made on the buildups of exponentially growing films.

Appendix

In this appendix, the height of the electrostatic barrier induced by the surface excess charge in the outer portion of the film is evaluated within the Debye−Hückel approximation. The excess charge is assumed to be located on the plane that separates the film from the solution. Let ρ^+ be the charge density on this plane and d the film thickness. The solution thus extends from d out to $+\infty$.

The first portion of the appendix treats the case of a film in contact with a pure salt (e.g., NaCl) solution of concentration ρ_0. Therefore, the solution does not contain polyelectrolyte chains and it is assumed that the same is true for the film. However, in general, the two polyelectrolyte species that comprise the film do not possess counterbalancing charges, so that a nonzero concentration of noncompensated "fixed" charges (ρ_{fc}) is present within the film. However, because the entire system must be electrically neutral, these "fixed" charges are compensated by counterions and result in a Donnan effect.[53] In the last portion of the appendix, we examine the more complex situation in which the film is brought into contact with a salt solution that contains a polyelectrolyte. In this case, it will be necessary to account for the polycations (or the polyanions) that penetrate into the film.

For linearly growing films, the driving force for buildup is the charge overcompensation that occurs after each new polyelectrolyte deposition.[1,2] The same observation has been made for exponentially growing films. At the end of each step, an excess charge appears in the outer portion of the multilayer.[15,36] A diffuse counterion charge at the outer layer compensates this excess. This cloud of counterions extends, in principle, into both the solution and the film over a characteristic screening length equal to the Debye length in each medium.[54] The counterion charges are, however, usually not evenly distributed between the solution and the film. The ratio between counterion charges in the film and solution is dependent on the dielectric constants of both media and on the ion concentrations deep in both the film and solution.

Charge Distribution in the Absence of Free Chains. The charge distribution ($\rho(z)$) results from the superposition of the excess charge at the interface, the charges carried by the ions (whatever their origin), and the charges that originate with the noncompensated polyions within the film. It is assumed that the charge distribution is dependent only on the distance z from the solid adsorbing surface at $z = 0$. It is related to the electrostatic potential ($V(z)$) by Poisson's equation. If the deposition substrate is planar, Poisson's equation reads

$$\frac{d^2V}{dz^2} = -\frac{\rho}{\epsilon_0\epsilon} \tag{A1}$$

where ϵ_0 is the dielectric constant of a vacuum and ϵ is the relative dielectric constant of the medium (film or solution). Provided that $\rho(z)$ is known, and taking the boundary conditions $V(+\infty) = 0$ and $(dV/dz)|_{z=+\infty} = 0$ into account, this equation can be integrated twice to yield the function $V(z)$. A schematic view of $\rho(z)$ and of the corresponding $V(z)$ is presented in Figure A1 for the particular case in which the charge of the polycations is exactly compensated within the film by the charge of the polyanions (for simplicity, the "fixed" charge concentration ρ_{fc} is taken equal to zero). Clearly, the excess charge located at the outermost portion of the film (i.e., at the film/solution interface) results in a maximum of V of the same sign. It follows that the interface constitutes an energy barrier for polycations. The larger the charge at the interface, the higher the energy barrier, which is a fact that will be confirmed quantitatively later by eq A19 with $\rho_{fc} = 0$. As in the body of the text, the superscripts "f" and "s" label quantities relative to the film and solution, respectively.

In the solution, the concentration of ions X (Na^+ or Cl^-) is given by

$$\rho_X^s = \rho_0 \exp\left(\pm\frac{eV(z)}{kT}\right) \tag{A2}$$

where the plus sign corresponds to Cl^- and the minus sign corresponds to Na^+, and e is the absolute value of the charge on an electron. The net charge density is

$$\rho^s = (\rho_{Na^+}^s - \rho_{Cl^-}^s)e \tag{A3}$$

It should be stressed that $\rho_{Na^+}^s$ and $\rho_{Cl^-}^s$ are concentrations and, thus, are positive numbers, whereas ρ^s is a charge density and can be either positive or negative. Introducing eqs A2 and A3 into eq A1 and assuming that $eV(z)/(kT) \ll 1$ leads to the classical one-dimensional linearized Poisson−Boltzmann equation. Its solution, which satisfies the aforementioned boundary conditions, is

$$V(z) = A^s \exp[-\kappa^s(z - d)] \tag{A4}$$

where A^s is a constant whose value is $V(d)$, i.e., at the film/solution interface. It also follows from the solution that the constant κ^s is defined by

$$\kappa^s = \sqrt{\frac{2\rho_0 e^2}{\epsilon^s\epsilon_0 kT}} \tag{A5}$$

and represents the reciprocal of the Debye length in a 1:1 electrolyte solution.[55]

The total charge density in the film (where, generally, $\rho_{fc} \neq 0$) is given by

$$\rho^f = (\rho_{fc} + \rho_{Na^+}^f - \rho_{Cl^-}^f)e \tag{A6}$$

We can define

$$\rho_X^f = \rho_{0,X}^f \exp\left(\pm\frac{eV(z)}{kT}\right) \tag{A7}$$

where $\rho_{0,X}^f$ is the concentration of ion X in the film, far from the interface, with the same sign convention as in eq A2. Note that, although ρ_{fc} is a concentration, it is a negative number if the "fixed" charges in the film are negative. The linearized Poisson−Boltzmann equation now takes the form

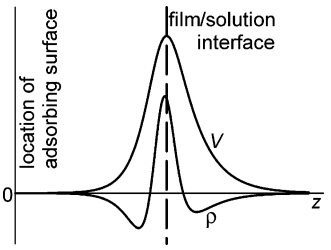

Figure A1. Behavior of the electrostatic potential (V) and of the charge distribution (ρ), as a function of the distance z from the substrate. Note the asymmetry of ρ—and, consequently, of V—which is due to the different values of the dielectric constant in the film and solution.

$$\epsilon_0\epsilon^f\frac{d^2V}{dz^2} = -(\rho_{fc} + \rho_{0,Na^+}^f - \rho_{0,Cl^-}^f)e + (\rho_{0,Na^+}^f + \rho_{0,Cl^-}^f)\frac{e^2V(z)}{kT} \tag{A8}$$

Note that, in contrast to the situation in the solution, the two types of ions are distinguished by separate symbols, because their concentrations in the film (even far from the interface) should not be considered equal on an a priori basis. The solution of eq A8 is

$$V(z) = A^f \exp[\kappa^f(z - d)] + U^f \tag{A9}$$

where U^f corresponds to the Donnan potential in the film and is independent of z. Inserting eq A9 into eq A8 leads to

$$U^f = \left[\frac{\rho_{fc} + \rho_{0,Na^+}^f - \rho_{0,Cl^-}^f}{(\rho_{0,Na^+}^f + \rho_{0,Cl^-}^f)e}\right]kT \tag{A10}$$

Furthermore, κ^f represents the reciprocal of the Debye length in the film and is given by

$$\kappa^f = \sqrt{\frac{(\rho_{Na^+}^f + \rho_{0,Cl^-}^f)e^2}{\epsilon_0\epsilon^f kT}} \tag{A11}$$

This expression is valid for a film thickness that is large, compared to the film Debye length.

Two continuity equations allow A^s and A^f to be determined. The first expresses the continuity of the electrostatic potential at $z = d$. The second originates from Gauss's theorem applied along the plane of excess charge. Thus, we have

$$\begin{cases} V(z = d^-) = V(z = d^+) \\ \epsilon^f\dfrac{dV}{dz}\Big|_{z=d^-} - \epsilon^s\dfrac{dV}{dz}\Big|_{z=d^+} = \dfrac{\rho^+}{\epsilon_0} \end{cases} \tag{A12}$$

where ρ^+ is the surface charge density (in units of C/m^2), which corresponds to the excess charge of the film. Introducing eqs A4 and A9 into eq A12 leads to

$$A^f = \frac{\rho^+ - \epsilon_0\epsilon^s\kappa^s U^f}{\epsilon_0(\epsilon^s\kappa^s + \epsilon^f\kappa^f)} \tag{A13a}$$

and

$$A^s = \frac{\rho^+ + \epsilon_0\epsilon^f\kappa^f U^f}{\epsilon_0(\epsilon^s\kappa^s + \epsilon^f\kappa^f)} \tag{A13b}$$

The expressions for U^f and κ^f, obtained previously, can be reformulated using the equality of ion electrochemical potentials in the film and the solution. These equalities read

$$\begin{cases} \mu^0_{Na^+} + kT \ln \rho_0 = \mu^0_{Na^+} + kT \ln \rho^f_{Na^+} + eU^f - kT \ln \varphi \\ \mu^0_{Cl^-} + kT \ln \rho_0 = \mu^0_{Cl^-} + kT \ln \rho^f_{Cl^-} - eU^f - kT \ln \varphi \end{cases} \quad \text{(A14)}$$

where μ^0_X corresponds to the chemical potential of ion X in the standard state and φ represents the available volume fraction per ion assumed to be the same for Na^+ and Cl^-. Note that we are neglecting the activity coefficients of the ions. Solving eq A14 leads to

$$\begin{cases} \rho^f_{Na^+} = \varphi\rho_0 \exp\left(-\dfrac{eU^f}{kT}\right) \\ \rho^f_{Cl^-} = \varphi\rho_0 \exp\left(\dfrac{eU^f}{kT}\right) \end{cases} \quad \text{(A15)}$$

The comparison of eq A15 with Eq A7 indicates that $V(z) \approx U^f$ deep in the film, in accordance with eq A9, and that the prefactor $\rho^f_{0,X}$ is equal to $\varphi\rho_0$. Inserting eq A15 into eq A6, and using the condition of local electroneutrality of the film far from the plane of excess charge, leads to

$$\rho_{fc} + \varphi\rho_0 \exp\left(-\frac{eU^f}{kT}\right) - \varphi\rho_0 \exp\left(\frac{eU^f}{kT}\right) = 0 \quad \text{(A16)}$$

This equation determines the Donnan potential U^f. In the framework of the Debye−Hückel approximation, i.e., $(eU^f/kT) \ll 1$, eq A16 gives the new expression for U^f. Thus,

$$U^f = \left(\frac{\rho_{fc}}{2\varphi\rho_0 e}\right)kT \quad \text{(A17)}$$

Note that this expression could have been obtained directly from eq A10 by replacing $\rho^f_{0,X}$ by $\varphi\rho_0$. This substitution also allows κ^f to be expressed by

$$\kappa^f = \sqrt{\frac{2\varphi\rho_0 e^2}{\epsilon_0 \epsilon^f kT}} \quad \text{(A18)}$$

The heights of the potential barriers as seen from the film, i.e., eq A13a, and from the solution, i.e., eq A13b, can then be rewritten in the forms

$$A^f = \frac{\rho^+ - (\rho_{fc}/\varphi)\sqrt{\epsilon_0\epsilon^s kT/(2\rho_0)}}{\sqrt{2\rho_0\epsilon_0 e^2/(kT)}\left(\sqrt{\epsilon^s} + \sqrt{\varphi\epsilon^f}\right)} \quad \text{(A19a)}$$

and

$$A^s = \frac{\rho^+ + (\rho_{fc}/\varphi)\sqrt{\epsilon_0\varphi\epsilon^f kT/(2\rho_0)}}{\sqrt{2\rho_0\epsilon_0 e^2/(kT)}\left(\sqrt{\epsilon^s} + \sqrt{\varphi\epsilon^f}\right)} \quad \text{(A19b)}$$

The maximum height, $\langle\Phi\rangle_{max}$, of the energy barrier introduced in eqs 4, 6, and 7 (see Section V) is proportional to the electrostatic potential A^s. Consequently, eq A19b shows that the energy barrier, as seen from the solution, decreases when the ionic strength, ρ_0, of the solution increases. Also, the barrier, as seen from the film, i.e., eq A19a, is reduced when the excess charge and the "fixed noncompensated" charges have the same sign. One may notice that when φ is small, the Debye length in the film, $1/\kappa^f$, can become large. We have assumed here that the film thickness is large, compared to $1/\kappa^f$. However, changes in the ionization of a polyelectrolyte that is deeply embedded in a multilayer, with only changes in the nature of the outer layer, were observed by Xie and Granick.[31] This finding can be explained as being due to a small value of φ, if the film thickness in these experiments was of the same order of magnitude as the Debye length of the film.

Charge Distribution in the Presence of Free Chains. In this portion of the appendix, we consider a film that is in contact with a solution that contains salt and polyelectrolyte. Furthermore, we assume that the film contains free polycations that penetrate into it through diffusion from the solution. In the present approach, we neglect the participation of the free polycations in the Debye length. This seems justified because the excess charge in the outer portion of the film always has the same sign as the free polycations in the film. Therefore, the electrostatic barrier repels the free polycation chains more strongly than the ions of same sign that have a much lower charge. Consequently, the chain concentration within the incompletely screened zone around the plane of excess charge should be rather small, especially when the Debye length is small, compared to the chain radius of gyration. Inside of the film, but beyond the screening distance, the polycation chain concentration should then be constant.

Let c^f and c^s be the respective polycation chain concentrations in the film and solution far from the film/solution interface and let N be the average number of charges carried by each chain. In a first approximation, the "free" chains in the film act as fixed charges.

When the film is in contact with a polycation solution at concentration c^s, the electroneutrality condition, in the solution far from the film, implies that

$$\rho^s_{0,Na^+} - \rho^s_{0,Cl^-} + Nc^s = 0 \quad \text{(A20)}$$

where $\rho^s_{0,X}$ represents the concentration of ions X in the solution, far from the interface. We assume that the pH of the solution is ~7, and, therefore, we neglect H^+ and OH^- ions. Equation A20 shows that, to compensate the positive charge Nc^se carried by the polycations, the concentration ρ^s_{0,Cl^-} must be larger than ρ^s_{0,Na^+}. This means that the solution must contain more Cl^- ions than Na^+ ions. These Cl^- ions may have as many as three origins: (i) the Cl^- ions associated with the polycations of the dissolved polyelectrolyte (e.g., PAH), (ii) the Cl^- ions from the HCl used for pH adjustment, and (iii) the Cl^- ions from the NaCl dissolved in the polyelectrolyte solution. One can thus write

$$\rho^s_{0,Cl^-} = \rho_0 + Nc^s \quad \text{(A21)}$$

where, as before, ρ_0 corresponds to the concentration of Cl^- introduced into the solution in the form of NaCl.

In the film, the electroneutrality equation, far from the interface, takes the form

$$\rho_{fc} + \rho^f_{0,Na^+} - \rho^f_{0,Cl^-} + Nc^f = 0 \quad \text{(A22)}$$

where $\rho^f_{0,X}$ is the concentration of ion X far from the interface. The ion number densities are given by equations that are similar to eq A15 when ρ_0 is replaced by $\rho^s_{0,X}$:

$$\begin{cases} \rho^{f}_{Na^+} = \varphi \rho^{s}_{0,Na^+} \exp\left(-\dfrac{eU^f}{kT}\right) \\ \rho^{f}_{Cl^-} = \varphi \rho^{s}_{0,Cl^-} \exp\left(\dfrac{eU^f}{kT}\right) \end{cases} \quad \text{(A23)}$$

The Donnan potential can be extracted from eq A22 using eq A23. Thus,

$$U^f = \left[\frac{\rho_{fc} + N(c^f - \varphi c^s)}{\varphi(2\rho_0 + Nc^s)e}\right]kT \quad \text{(A24)}$$

Inserting this expression for U^f into the general equations (eqs A13a,b) yields the electrostatic potential barriers:

$$A^f = \frac{\rho^+}{\epsilon_0(\epsilon^s\kappa^s + \epsilon^f\kappa^f)} - \frac{\epsilon^s\kappa^s(\rho_{fc} + Nc^f - N\varphi c^s)kT}{\varphi(\epsilon^s\kappa^s + \epsilon^f\kappa^f)(2\rho_0 + Nc^s)e} \quad \text{(A25a)}$$

and

$$A^s = \frac{\rho^+}{\epsilon_0(\epsilon^s\kappa^s + \epsilon^f\kappa^f)} + \frac{\epsilon^f\kappa^f(\rho_{fc} + Nc^f - N\varphi c^s)kT}{\varphi(\epsilon^s\kappa^s + \epsilon^f\kappa^f)(2\rho_0 + Nc^s)e} \quad \text{(A25b)}$$

where κ^s and κ^f are still given by eqs A5 and A18, respectively, because the effect of the polycations is neglected in their expression.

Now, we determine the concentration of free chains in the film when equilibrium is reached between the film and the polycation solution. Because the electrostatic potential is zero deep within the solution, the electrochemical potentials of a polycation are given by

$$\begin{cases} \mu^s = \mu^{0,s} + kT \ln c^s \\ \mu^f = \mu^{0,f} + NeU^f + kT \ln c^f - kT \ln \varphi' \end{cases} \quad \text{(A26)}$$

where μ^0 represents the kinetic and entropic contributions, as well as the interactions of the chains with water. In eq A26, φ' corresponds to the available volume fraction for the polycation. At equilibrium, the electrochemical potentials are equal in the film and solution. Thus, from eq A26, we have

$$c^s = \frac{c^f}{\varphi'} \exp\left[N\left(\frac{eU^f}{kT}\right)\right] \exp\left(\frac{\mu^{0,f} - \mu^{0,s}}{kT}\right) \quad \text{(A27)}$$

Assume that $\mu^{0,f}$ and $\mu^{0,s}$ are of the same order of magnitude. The second exponential in eq A27 then is on the order of unity. Replacing, in eq A27, U^f by its value given by eq A24 leads to

$$\varphi c^s \exp\left[\left(\frac{N^2}{2\varphi\rho_0}\right)\varphi c^s\right] = Fc^f \exp\left[\left(\frac{N^2}{2\varphi\rho_0}\right)c^f\right] \quad \text{(A28)}$$

with

$$F = \frac{\varphi}{\varphi'} \exp\left(\frac{N\rho_{fc}}{2\varphi\rho_0}\right) \quad \text{(A29)}$$

where we have assumed that $Nc^s \ll 2\rho_0$. If a polyanion, instead of a polycation, diffuses in the film, eq A28 remains valid but the constant F becomes

$$F = \frac{\varphi}{\varphi'} \exp\left(-\frac{N\rho_{fc}}{2\varphi\rho_0}\right) \quad \text{(A30)}$$

The form of c^f, as a function of φc^s, can be deduced from eq A28.

Acknowledgment. We thank Prof. G. D. Prestwich (Department of Medical Chemistry, University of Utah) for his work on HA modification and for fruitful discussions. This work was supported by the programs ACI "Technologies pour la Santé" and "Surfaces, Interfaces et Conception de Nouveaux Matériaux" (from the Ministère Français de la Recherche), by the European Community through the SIMI program, and by the CNRS program "Physique et Chimie du Vivant". Ph.L. is indebted to the Institut Français pour la Recherche Odontologique for financial support. The CLSM platform used in this study was co-financed by the Région Alsace, the CNRS, the Université Louis Pasteur, and the Association pour la Recherche sur le Cancer. H.R. acknowledges the financial support of the NSF (Grant No. CHE-0301356).

References and Notes

(1) Caruso, F.; Lichtenfeld, H.; Donath, E.; Möhwald, H. *Macromolecules* **1999**, *32*, 2317−2328.
(2) Ladam, G.; Schaad, P.; Voegel, J.-C.; Schaaf, P.; Decher, G.; Cuisinier, F. J. G. *Langmuir* **2000**, *16*, 1249−1255.
(3) Decher, G. *Science* **1997**, *277*, 1232−1237.
(4) Fou, A. C.; Onitsuka, O.; Ferreira, M.; Rubner, M. F.; Hsieh, B. R. *J. Appl. Phys.* **1996**, *79*, 7501−7509.
(5) Eckle, M.; Decher, G. *Nano Lett.* **2001**, *1*, 45−49.
(6) Mendelsohn, J. D.; Yang, S. Y.; Hiller, J.; Hochbaum, A.; Rubner, M. F. *Biomacromolecules* **2003**, *4*, 96−106.
(7) Serizawa, T.; Yamaguchi, M.; Akashi, M. *Biomacromolecules* **2002**, *3*, 724−731.
(8) Chluba, J.; Voegel, J.-C.; Decher, G.; Erbacher, P.; Schaaf, P.; Ogier, J. *Biomacromolecules* **2001**, *2*, 800−805.
(9) Elbert, D. L.; Herbert, C. B.; Hubbell, J. A. *Langmuir* **1999**, *15*, 5355−5362.
(10) Lvov, Y.; Caruso, F. *Anal. Chem.* **2001**, *73*, 4212−4217.
(11) Schlenoff, J. B.; Dubas, S. T. *Macromolecules* **2001**, *34*, 592−598.
(12) Mendelsohn, J. D.; Barrett, C. J.; Chan, V. V.; Pal, A. J.; Mayes, A. M.; Rubner, M. F. *Langmuir* **2000**, *16*, 5017−5023.
(13) Shiratori, S. S.; Rubner, M. F. *Macromolecules* **2000**, *33*, 4213−4219.
(14) Xie, A. F.; Granick, S. *J. Am. Chem. Soc.* **2001**, *123*, 3175−3176.
(15) Picart, C.; Lavalle, P.; Hubert, P.; Cuisinier, F. J. G.; Decher, G.; Schaaf, P.; Voegel, J.-C. *Langmuir* **2001**, *17*, 7414−7424.
(16) Picart, C.; Mutterer, J.; Richert, L.; Luo, Y.; Prestwich, G. D.; Schaaf, P.; Voegel, J.-C.; Lavalle, P. *Proc. Natl. Acad. Sci. U.S.A.* **2002**, *99*, 12531−12535.
(17) von Klitzing, R.; Möhwald, H. *Langmuir* **1995**, *11*, 3554−3559.
(18) Kovacevic, D.; van der Burgh, S.; de Keizer, A.; Cohen Stuart, M. A. *Langmuir* **2002**, *18*, 5607−5612.
(19) Castelnovo, M.; Joanny, J. F. *Langmuir* **2000**, *16*, 7524−7532.
(20) Park, S. Y.; Barrett, C. J.; Rubner, M. F.; Mayes, A. M. *Macromolecules* **2001**, *34*, 3384−3388.
(21) Finkenstadt, D.; Johnson, D. D. *Langmuir* **2002**, *18*, 1433−1436.
(22) Park, S. Y.; Rubner, M. F.; Mayes, A. M. *Langmuir* **2002**, *18*, 9600−9604.
(23) Yoo, D.; Shiratori, S. S.; Rubner, M. F. *Macromolecules* **1998**, *31*, 4309−4318.
(24) Arys, X.; Laschewsky, A.; Jonas, A. M. *Macromolecules* **2001**, *34*, 3318−3330.
(25) Caruso, F.; Niikura, K.; Furlong, D. N.; Okahata, Y. *Langmuir* **1997**, *13*, (3), 3422−3426.
(26) Ramsden, J. J.; Lvov, Y. M.; Decher, G. *Thin Solid Films* **1995**, *254*, 246−251.
(27) Picart, C.; Ladam, G.; Senger, B.; Voegel, J.-C.; Schaaf, P.; Cuisinier, F. J. G.; Gergely, C. *J. Chem. Phys.* **2001**, *115*, 1086−1094.
(28) Ruths, J.; Essler, F.; Decher, G.; Riegler, H. *Langmuir* **2000**, *16*, 8871−8878.
(29) Korneeva, D.; Lvov, Y.; Decher, G.; Schmitt, J.; Yaradaikin, S. *Physica B* **1995**, *213−214*, 954−956.
(30) Steitz, R.; Leiner, V.; Siebrecht, R.; Klitzing, R. V. *Colloid Surf. A* **2000**, *163*, 63−70.
(31) Xie, A. F.; Granick, S. *J. Am. Chem. Soc.* **2001**, *123*, 3175−3176.
(32) Sui, Z. J.; Salloum, D.; Schlenoff, J. B. *Langmuir* **2003**, *19*, 2491−2495.
(33) Glinel, K.; Moussa, A.; Jonas, A. M.; Laschewsky, A. *Langmuir* **2002**, *18*, 1408−1412.
(34) McAloney, R. A.; Sinyor, M.; Dudnik, V.; Goh, M. C. *Langmuir* **2001**, *17*, 6655−6663.

(35) Pardo-Yissar, V.; Katz, E.; Lioubashevski, O.; Willner, I. *Langmuir* **2001**, *17*, 1110−1118.
(36) Lavalle, P.; Gergely, C.; Cuisinier, F. J. G.; Decher, G.; Schaaf, P.; Voegel, J.-C.; Picart, C. *Macromolecules* **2002**, *35*, 4458−4465.
(37) Schoeler, B.; Poptoshev, E.; Caruso, F. *Macromolecules* **2003**, *36*, 5258−5264.
(38) DeLongchamp, D. M.; Kastantin, M.; Hammond, P. T. *Chem. Mater*. **2003**, *15*, 1575−1586.
(39) Boulmedais, F.; Schwinté, P.; Gergely, C.; Voegel, J.-C.; Schaaf, P. *Langmuir* **2002**, *18*, 4523−4525.
(40) Boulmedais, F.; Ball, V.; Schwinté, P.; Frisch, B.; Schaaf, P.; Voegel, J.-C. *Langmuir* **2003**, *19*, 440−445.
(41) Jessel, N.; Atalar, F.; Lavalle, P.; Mutterer, J.; Decher, G.; Schaaf, P.; Voegel, J. C.; Ogier, J. *Adv. Mater*. **2003**, *15*, 692−695.
(42) Ramsden, J. J. *J. Mol. Recognit.* **1997**, *10*, 109−120.
(43) Tiefenthaler, K.; Lukosz, W. *J. Opt. Soc. Am. B.* **1989**, *6*, 209−220.
(44) Rodahl, M.; Kasemo, B. *Rev. Sci. Instrum.* **1996**, *67*, 3238−3241.
(45) Hook, F.; Rodahl, M.; Brzezinski, P.; Kasemo, B. *J. Colloid Interface Sci.* **1998**, *208*, 63−67.
(46) Picart, C., unpublished data, 2003.
(47) Murphy, W. D.; Rabeony, H. M.; Reiss, H. *J. Phys. Chem.* **1988**, *22*, 7007.
(48) Schlenoff, J.; Ly, H.; Li, M. *J. Am. Chem. Soc.* **1998**, *120*, 7626−7634.
(49) Hoogeveen, N. G.; Cohen-Stuart, M. A.; Fleer, G. J.; Böhmer, M. R. *Langmuir* **1996**, *12*, 3675−3681.
(50) Kovacevic, D.; van der Burgh, S.; de Keizer, A.; Cohen-Stuart, M. A. *Langmuir* **2002**, *18*, 5607−5612.
(51) de Groot, S. R.; Mazur, P. *Nonequilibrium Thermodynamics*; Dover: New York, 1984.
(52) Adamczyk, Z.; Senger, B.; Voegel, J.-C.; Schaaf, P. *J. Chem. Phys.* **1999**, *110*, 3118−3128.
(53) Helfferich, F. *Ion Exchange*; McGraw−Hill: New York, 1962.
(54) Klitzing, R. V.; Möhwald, H. *Langmuir* **1995**, *11*, 3554−3559.
(55) Israelachvili, J. *Intermolecular and Surface Forces*; Academic Press: London, 1992.